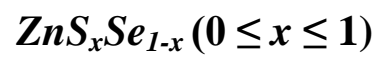


COMPUTATIONAL AND THEORETICAL STUDIES ON



GHASSAN H. ESA AL-SHABEEB

**FACULTY OF SCIENCE
UNIVERSITY OF MALAYA
KUALA LUMPUR**

2012

COMPUTATIONAL AND THEORETICAL STUDIES ON
 ZnS_xSe_{1-x} ($0 \leq x \leq 1$)

GHASSAN H. ESA AL-SHABEEB

THESIS SUBMITTED FOR THE DEGREE OF
DOCTOR OF PHILOSOPHY

DEPARTMENT OF PHYSICS
FACULTY OF SCIENCE
UNIVERSITY OF MALAYA
KUALA LUMPUR

2012

LIST OF PUBLICATIONS

1. **Ghassan H.E. Al-Shabeeb** and A.K. Arof (2010). Energy Gap Calculations for ZnS_xSe_{1-x} , National Physics Conference PERFIK 2009, 7-9 Dec. 2009, *AIP Conf. Proc.* **1250**, pp.97-100. (ISI)
2. **Ghassan H.E. Al-Shabeeb** and A.K. Arof (2010). Electron Energy Spectrum in II–VI Materials: Simplified Theory, Second International Conference on Computer Research and Development 2010 IEEE, *ICCRD Proc.*2010.**131**, pp. 611-614. (ISI)
3. **Ghassan H.E. Al-Shabeeb** and A.K. Arof, (2011), Theoretical Studies on the Energy Gap Variation in ZnS_xSe_{1-x} , ($0 \leq x \leq 1$), *Materials Research Innovations* 15, S2 132-136.(ISI)

ABSTRACT

The aim of this work is to study a theory of the energy band gap of ZnS_xSe_{1-x} ($0 \leq x \leq 1$) materials, and to obtain the density of states (DOS) in a quantizing magnetic field. From $\vec{k} \cdot \vec{p}$ perturbation theory, momentum matrix elements and energy eigenvalue of the Zn-S-Se alloy are derived. An empirical relationship $\frac{\mu^*}{m_c} = (0.124Eg_0)^{1.76}$ where $(\mu^*)^{-1} = (m_c)^{-1} + (m_v)^{-1}$, and m_c , m_v are the electron and hole rest masses respectively, is incorporated in the derivation of the energy gap equation

$$Eg = Eg_0 + \frac{2\hbar^2\pi^2}{m_c D^2 \left((0.124Eg_0)^{1.76} \right)}$$

The $\vec{k} \cdot \vec{p}$ perturbation theory is also extended to include the spin-orbit interaction leading to a different expression for the energy gap

$$Eg = Eg_0 + \frac{2\hbar^2\pi^2}{D^2 \left((0.124Eg_0)^{1.76} \right) m_c \left(Eg_0 + \frac{2}{3}\Delta \right)} \frac{(Eg_0 + \Delta)}{\left(Eg_0 + \frac{2}{3}\Delta \right)}$$

Third, the density of states (DOS) for ZnS_xSe_{1-x} in a quantizing magnetic field has been determined by the E-k relation. The energy gap calculated from CASTEP is considered the unperturbed energy gap, Eg_0 . The actual energy Eg is related to Eg_0 and results obtained are in reasonable agreement with published results obtained from literature. Energy gap with spin-orbit interaction is higher than the values calculated using energy gap equation without spin.

The DOS

$$N(E) = \frac{1}{4\pi^2} \left(\frac{2m_c}{\hbar^2} \right)^{3/2} \frac{\hbar eB}{m_c} \left[E - \left((0.124Eg_0)^{1.76} \right) \frac{(l + (1/2))\hbar eB}{\mu^*} \right]^{1/2}$$

is shown to depend on the electron energy and the magnetic field. Fermi level is modified by the magnetic field.

ABSTRAK

Tujuan kerja ini adalah untuk membangunkan teori jurang jalur tenaga bahan-bahan ZnS_xSe_{1-x} ($0 \leq x \leq 1$), dan untuk mendapatkan ketumpatan keadaan (DOS) dalam medan magnet pengkuantuman. Menurut teori pertubasi $\vec{k} \cdot \vec{p}$, matriks momentum unsur-unsur dan nilai tenaga eigen aloi Zn-S-Se diperolehi. Hubungan empirikal di mana $(\mu^*)^{-1} = (m_c)^{-1} + (m_v)^{-1}$, dengan m_c dan m_v masing-masing adalah jisim elektron dan jisim lohong dimuatkan dalam menerbitkan persamaan jurang tenaga.

$$E_g = E_{g_0} + \frac{2\hbar^2\pi^2}{m_c D^2 \left((0.124 E_{g_0})^{1.76} \right)}$$

Teori pertubasi $\vec{k} \cdot \vec{p}$ juga diperluaskan kepada interaksi spin-orbit yang membawa kepada ungkapan yang berlainan bagi persamaan jurang tenaga

$$E_g = E_{g_0} + \frac{2\hbar^2\pi^2}{D^2 \left((0.124 E_{g_0})^{1.76} \right) m_c} \frac{(E_{g_0} + \Delta)}{\left(E_{g_0} + \frac{2}{3}\Delta \right)}$$

Ketiga, ketumpatan keadaan (DOS) untuk ZnS_xSe_{1-x} dalam medan magnet pengkuantuman telah ditentukan oleh hubungan E - k . Jurang tenaga yang ditaksir dari CASTEP dianggap jurang tenaga tidak terusik, E_{g_0} . Tenaga jalur tidak terusik adalah berkaitan dengan E_{g_0} dan keputusan yang diperolehi adalah munasabah dengan hasil yang telah diterbitkan dalam jurnal. Jurang tenaga dengan interaksi spin-orbit adalah lebih tinggi daripada nilai-nilai dikira menggunakan persamaan jurang tenaga tanpa spin-orbit.

DOS

$$N(E) = \frac{1}{4\pi^2} \left(\frac{2m_c}{\hbar^2} \right)^{3/2} \frac{\hbar e B}{m_c} \left[E - \left((0.124 E_{g_0})^{1.76} \right) \frac{(1 + (1/2)) \hbar e B}{\mu^*} \right]^{1/2}$$

ditunjukkan bergantung kepada tenaga elektron dan medan magnet. Aras Fermi diubahsuai oleh medan magnet.

ACKNOWLEDGMENT

First and foremost, I would like to thank my supervisor, Prof. Dr. Abdul Kariem Bin Mohd Arof for his continuous guidance and support throughout this work, without him this thesis would never have been written.

I am grateful to Mr. Faris and Mr. Muhammad Kamil of the University Technology Mara for providing the Materials Studio computer program. I also express my gratitude to Mr. Ahamad Nazrul Bin Rosli and Ms. Noriza Binti Ahmad Zabidi for their support. I express my gratitude to all my friends in advanced material lab.

Without the support of my family, friends and my lovely daughters Zainab and Umaima this thesis would never have been completed. Thanks to you all.

This work is supported by the University of Malaya, PPP grant (Project No. PS320/2009B and PS331/2010A). I am grateful to the authorities of the University of Malaya for encouragements, and for giving me the opportunity to study in this great university.

Last but not the least; I thank the authorities of the University of Malaya for giving me the opportunity to study in this great university.

CONTENTS

List of publication	i
Abstract	ii
Abstrak	iii
Acknowledgments	iv
Contents	v
List of Figures	viii
List of Tables	xii
CHAPTER 1: Introduction To The Thesis	
1.1 Objective	3
1.2 Outline Of Thesis	3
CHAPTER 2: Literature Review	
2.1 Introduction	6
2.2 The Energy Bands	7
2.3 Brillouin Zone	12
2.4 Normal Form Of An Energy Band	15
2.5 ZnS_xSe_{1-x} ($0 \leq x \leq 1$) as II-VI Compounds Crystal Structure	18
2.6 Effective Mass	24
2.7 Reduced Mass	25
2.8 Physical Properties Of The ZnS And $ZnSe$ Compounds	26
2.9 Band Gaps For ZnS_xSe_{1-x} ($0 \leq x \leq 1$)	28
2.10 Schrödinger Equation	31
2.11 Perturbation Theory	33
2.12 $\vec{k} \cdot \vec{p}$ Theory	34

2.13 Spin-Orbit Interaction	36
2.14 Effect Of Large Magnetic Fields	38
2.15 The Density Of States Function	38
2.16 Density Functional Theory From Wave Functions To Electron Density	40
2.16.1 Local-Density Approximation (LDA)	42
2.16.2 Local-Spin-Density Approximation (LSDA)	43
2.16.3 Generalized Gradient Approximation (GGA)	44
2.17 Cambridge Serial Total Energy Package (CASTEP)	45
2.17.1 Exchange-Correlation Functional	46
2.17.2 Pseudopotential	47
2.17.3 Self-Consistent Electrons Minimization	47
2.18 Summary	48

CHAPTER 3: Results For ZnS_xSe_{1-x} ($0 \leq x \leq 1$) From CASTEP

3.1 Introduction	51
3.2 Computational Method	52
3.3 Computational Results	55
3.3.1 ZnS Band Structure Calculation	55
3.3.2 ZnSe Band Structure Calculation	57
3.3.3 $ZnS_{0.125}Se_{0.875}$ Band Structure Calculation	60
3.3.4 $ZnS_{0.25}Se_{0.75}$ Band Structure Calculation	62
3.3.5 $ZnS_{0.375}Se_{0.625}$ Band Structure Calculation	64
3.3.6 $ZnS_{0.5}Se_{0.5}$ Band Structure Calculation	67
3.3.7 $ZnS_{0.625}Se_{0.375}$ Band Structure Calculation	69
3.3.8 $ZnS_{0.75}Se_{0.25}$ Band Structure Calculation	71
3.3.9 $ZnS_{0.875}Se_{0.125}$ Band Structure Calculation	74

3.4	Summary	77
CHAPTER 4: Results On Energy Gap For ZnS_xSe_{1-x} ($0 \leq x \leq 1$): A Simple Theory		
4.1	The Spinless $\vec{k}\cdot\vec{p}$ Perturbation	79
4.2	Results	86
4.3	Summary	90
CHAPTER 5: Results On Energy Gap For ZnS_xSe_{1-x}: The Effect Of Spin-Orbit Interaction		
5.1	Introduction	92
5.2	Coupling Of Spin And Orbital Angular Momentum	93
5.3	The $\vec{k}\cdot\vec{p}$ Perturbation Theory With The Effect Of Spin-Orbitinteraction	95
5.4	Results	112
5.5	Summary	115
CHAPTER 6: Results On The Density Of States For ZnS_xSe_{1-x} In The Presence Of Quantizing Magnetic Field		
6.1	Introduction	117
6.2	The Formulation Of The Dos For The II–VI Materials In The Presence Of A Quantizing Magnetic Field	119
6.3	The Effect Of Magnetic Field On The Fermi Level In The Case Of Parabolic Band	123
6.4	Results	125
6.5	Summary	128
CHAPTER 7: Discussion		130
CHAPTER 8: Conclusions And Suggestions For Future Work		148
REFERENCES		151
APPENDIX A		160

LIST OF FIGURES

Figure 2.1	Simplified diagram of the electronic band structure of metals, semi- conductors, and insulators.	7
Figure 2.2	Schematic electron occupancy of allowed energy bands for (a) metal, (b) semiconductor and (c) insulator which is showing no gap, narrow and wide band gap respectively. The metal has half filled conduction band, the insulator has no population in the conduction band and the semiconductor has a very small population of electrons [Kittle, 1996].	8
Figure 2.3	Semiconductor band structure.	9
Figure 2.4	The first and second Brillouin zones of a two-dimensional square lattice.	13
Figure 2.5	The lattice vectors for fcc primitive cell of (a) real space where atoms is represented by circles and (b) reciprocal space with basis vectors are shown inside a cube with side length $4^{1/4}/a$ centered at the origin [Sholl and Steckel, 2009].	14
Figure 2.6	Standard labels of the symmetry and axes of the Brillouin zone of the face centred cubic (fcc), body centred cubic (bcc), simple cubic and hexagonal lattices where Γ is the zone centres [Kittel, 1996].	16
Figure 2.7	Crystal structure of sphalerite for ZnS with space group F-43M (TD-2). The lattice parameters for ZnS sphalerite crystal structure are $a=5.41 \text{ \AA}$ [Aswegen and Verleger, 1960].	18
Figure 2.8	Crystal structure of sphalerite for ZnSe with space group F-43M (TD-2). The lattice parameter for ZnSe sphalerite crystal structure $a=5.6686\pm 0.006 \text{ \AA}$ [Goryunova and Fedorova, 1959].	19
Figure 2.9	Crystal structure of wurtzite for ZnS with space group P63mc. The lattice parameter for wurtzite crystal structure $a=3.82 \text{ \AA}$, $c=6.26 \text{ \AA}$ [Hansen and Andreko, 1968], for ZnSe the lattice parameter in case of wurtzite crystal structure are $a=4.01\pm 0.02 \text{ \AA}$, $c=6.54\pm 0.02 \text{ \AA}$ [Pashinkin et al., 1960; Goryunova and Fedorova, 1959].	19
Figure 2.10	Crystal structure of sphalerite for $ZnS_{0.125}Se_{0.875}$ with space group P-42M (D2D-1) and lattice parameter $a=b=5.4093 \text{ \AA}$, $c=10.8186 \text{ \AA}$ [CASTEP simulation].	20

Figure 2.11	Crystal structure of sphalerite for $ZnS_{0.25}Se_{0.75}$ with space group P-4M2 (D2D-5) and lattice parameter $a=b=5.4093 \text{ \AA}$, $c=10.8186 \text{ \AA}$ [CASTEP simulation].	20
Figure 2.12	Crystal structure of sphalerite for $ZnS_{0.375}Se_{0.625}$ with space group CMM2 (C2V-11) and lattice parameter $a=b=5.4093 \text{ \AA}$, $c=10.8186 \text{ \AA}$ [CASTEP simulation].	21
Figure 2.13	Crystal structure of sphalerite for $ZnS_{0.5}Se_{0.5}$ with space group P-4M2 (D2D5) and lattice parameter $a=b=5.4093 \text{ \AA}$, $c=10.8186 \text{ \AA}$ [CASTEP simulation].	21
Figure 2.14	Crystal structure of sphalerite for $ZnS_{0.75}Se_{0.25}$ with space group CMME (C2V-11) and lattice parameter $a=b=5.4093 \text{ \AA}$, $c=10.8186 \text{ \AA}$ [CASTEP simulation].	22
Figure 2.15	$CsCl$ crystal structure [Slyusarenko, 2008].	23
Figure 2.16	Constant energy ellipsoids in silicon near the six conduction band minima. The longitudinal and transverse effective masses are $m_l = 0.92 m$ and $m_t = 0.19 m$ with m the free electron mass [Kittel, 1996].	24
Figure 2.17	Concentric shells in k-space used to evaluate the DOS, $g(E)$ [Erkoç and Uzer, 1996].	40
Figure 2.18	The local density approximation [Koch and Holthausen, 2001].	43
Figure 3.1	Brillouin zone for ZnS crystal structure in simple cubic.	56
Figure 3.2	The calculated energy band structure for ZnS .	56
Figure 3.3	Total density of states for ZnS .	57
Figure 3.4	Brillouin zone for $ZnSe$ crystal structure in simple cubic.	58
Figure 3.5	The calculated energy band structure for $ZnSe$.	58
Figure 3.6	Total density of states for $ZnSe$.	59
Figure 3.7	Brillouin zone for $ZnS_{0.125}Se_{0.875}$ crystal structure.	60
Figure 3.8	The calculated energy band structure for $ZnS_{0.125}Se_{0.875}$.	61
Figure 3.9	Total density of states for $ZnS_{0.125}Se_{0.875}$.	61
Figure 3.10	Brillouin zone for $ZnS_{0.25}Se_{0.75}$ crystal structure.	62
Figure 3.11	The calculated energy band structure for $ZnS_{0.25}Se_{0.75}$.	63

Figure 3.12	Total density of states for $ZnS_{0.25}Se_{0.75}$.	64
Figure 3.13	Brillouin zone for $ZnS_{0.375}Se_{0.625}$ crystal structure.	65
Figure 3.14	The calculated energy band structure for $ZnS_{0.375}Se_{0.625}$.	65
Figure 3.15	Total density of states for $ZnS_{0.375}Se_{0.625}$.	66
Figure 3.16	Brillouin zone for $ZnS_{0.5}Se_{0.5}$ crystal structure.	67
Figure 3.17	The calculated energy band structure for $ZnS_{0.5}Se_{0.5}$.	68
Figure 3.18	Total density of states for $ZnS_{0.5}Se_{0.5}$.	69
Figure 3.19	Brillouin zone for $ZnS_{0.625}Se_{0.375}$ crystal structure. (with space group CMM2(C2V-11)).	70
Figure 3.20	The calculated energy band structure for $ZnS_{0.625}Se_{0.375}$.	70
Figure 3.21	Total density of states for $ZnS_{0.625}Se_{0.375}$.	71
Figure 3.22	Brillouin zone for $ZnS_{0.75}Se_{0.25}$ crystal structure.	72
Figure 3.23	The calculated energy band structure for $ZnS_{0.75}Se_{0.25}$.	73
Figure 3.24	Total density of states for $ZnS_{0.75}Se_{0.25}$.	74
Figure 3.25	Brillouin zone for $ZnS_{0.875}Se_{0.125}$ crystal structure.	75
Figure 3.26	The calculated energy band structure for $ZnS_{0.875}Se_{0.125}$.	75
Figure 3.27	Total density of states for $ZnS_{0.875}Se_{0.125}$.	76
Figure 3.28	E_g as a function of x from CASTEP computation upon applying the 1.7 and 1.66 multiplicative correction factors.	77
Figure 4.1	E_g as a function of x upon applying the 1.7 correction factor.	89
Figure 4.2	E_g as a function of x upon applying the 1.66 correction factor.	89
Figure 4.3	E_g as a function of x from Larach <i>et al.</i> , [1974], Abo Hassan <i>et al.</i> , [2005a], and the results for this work.	90
Figure 5.1	Spin orbit splitting constant with various x for ZnS_xSe_{1-x} for sphalerite crystal structure.	112
Figure 5.2	Spin orbit splitting constant with various x for ZnS_xSe_{1-x} for wurtzite crystal structure.	113

Figure 5.3	E_g as a function of a concentration x for ZnS_xSe_{1-x} upon applying the 1.7 correction factor in case of wurtzite crystal structure, sphalerite crystal structure, and E_g without spin.	114
Figure 5.4	E_g as a function of a concentration x for ZnS_xSe_{1-x} upon applying the 1.66 correction factor in case of wurtzite crystal structure, sphalerite crystal structure, and E_g without spin.	114
Figure 5.5	E_g as a function of a concentration x for ZnS_xSe_{1-x} upon applying the 1.7 and 1.66 correction factors in case of wurtzite crystal structure, sphalerite crystal structure, E_g without spin, experimental results reported by Larach <i>et al.</i> [1957] and Abo Hassan <i>et al.</i> [2005a].	115
Figure 6.1	Density of states as a function of electron energy for ZnS ($B=0.1, 0.5, 0.75, 1$ Tesla and $l=1$).	126
Figure 6.2	Density of states as a function of electron energy for $ZnSe$ ($B=0.1, 0.5, 0.75, 1$ Tesla and $l=1$).	126
Figure 6.3	Density of states as a function of electron energy for ZnS_xSe_{1-x} ($x=0.9$) ($B=0.1, 0.5, 0.75, 1$ Tesla and $l=1$).	127
Figure 6.4	Density of status as a function of x . ($0 < x < 1$) for $B= 0.5, 0.75, 1$ Tesla, and $E=1eV$.	127
Figure 6.5	n/N_c as a function of $\eta - \varphi/2$, showing the effect of magnetic field on the Fermi level for a constant electron concentration.	128

LIST OF TABLES

Table 2.1	The notations, used to label the critical points of the symmetry and axes of the Brillouin zone.	17
Table 2.2	Electrical Properties of ZnS and $ZnSe$ compounds.	27
Table 2.3	Energy band gaps for ZnS_xSe_{1-x} ($0 \leq x \leq 1$).	29
Table 3.1	Calculated equilibrium lattice parameters, internal parameter u for ZnS_xSe_{1-x} [Mesri <i>et al.</i> , 2007].	54
Table 4.1	Shift in band gap ΔEg caused by grain size effect and reduce effective mass μ^* for ZnS_xSe_{1-x} ($0 < x < 1$) thin films.	85
Table 4.2	D values for ZnS_xSe_{1-x} [Abo Hassan <i>et al.</i> , 2005b].	87
Table 4.3	Energy gap Eg from this work upon applying the 1.7 correction factor.	88
Table 4.4	Energy gap Eg from this work upon applying the 1.66 correction factor.	88
Table 7.1	Comparing results for energy band gaps for ZnS_xSe_{1-x} ($0 \leq x \leq 1$).	140
Table 7.2	Spin-orbit splitting constant for sphalerite and wurtzite crystal structures with density of states for ZnS_xSe_{1-x} ($0 < x < 1$).	143